© 2016. Published by The Company of Biologists Ltd | Journal of Experimental Biology (2016) 219, 1259-1268 doi:10.1242/jeb.133181

RESEARCH ARTICLE

CHHBP: a newly identified receptor of crustacean hyperglycemic hormone

Ran Li[1], Jin-Ze Tian[1], Cui-Heng Zhuang[1], Yi-Chen Zhang[1], Xu-Yun Geng[2], Li-Na Zhu[1] and Jin-Sheng Sun[1,2,*]

ABSTRACT

Crustacean hyperglycemic hormone (CHH) is a neurohormone found only in arthropods that plays a pivotal role in the regulation of hemolymph glucose levels, molting and stress responses. Although it was determined that a membrane guanylyl cyclase (GC) acts as the CHH receptor in the Y-organ during ecdysteroidogenesis, the identity of the CHH receptor in the hepatopancreas has not been established. In this study, we identified CHH binding protein (CHHBP), as a potential receptor by screening the annotated unigenes from the transcriptome of *Eriocheir sinensis*, after removal of the eyestalk. Analysis of the binding affinity between CHH and CHHBP provided direct evidence that CHH interacts with CHHBP in a specific binding mode. Subsequent analysis showed that CHHBP is expressed primarily in the hepatopancreas where it localizes to the cell membrane. In addition, real-time PCR analysis showed that *CHHBP* transcript levels gradually increase in the hepatopancreas following eyestalk ablation. RNAi-mediated suppression of *CHHBP* expression resulted in decreased glucose levels. Furthermore, the reduction of blood glucose induced by *CHHBP* RNAi reached the same level as that observed in the eyestalk ablation group, suggesting that CHHBP is involved in glucose metabolism regulated by CHH. In addition, compared with the control group, injection of CHH was unable to rescue the decreased glucose levels in *CHHBP* RNAi crabs. CHH induced transport of 2-NBDG to the outside of cells, with indispensable assistance from CHHBP. Taken together, these findings suggest that CHHBP acts as one type of the primary signal processor of CHH-mediated regulation of cellular glucose metabolism.

KEY WORDS: Glucose metabolism, Hormone receptor, Cell signaling, Protein–protein interaction, Cell surface receptor, Crustacean hyperglycemic hormone, *Eriocheir sinensis*

INTRODUCTION

Crustacean hyperglycemic hormone (CHH) belongs to the CHH neuropeptide family. This family consists of CHH and its structurally related peptides, including molt-inhibiting hormone (MIH), vitellogenesis/gonad-inhibiting hormone (VIH/GIH) and mandibular organ-inhibiting hormone (MOIH) in crustaceans, and ion transport peptide (ITP) in insects. Thus far, CHH family members have been identified only in arthropods and ecdysozoans (Montagné et al., 2010; Webster et al., 2012).

It is now widely appreciated that CHH is a pleiotropic hormone that plays a pivotal role in the regulation of several physiological activities, such as maintaining hemolymph glucose levels, lipid metabolism, molting and the stress response (Webster et al., 2012). The first described role of CHH was in the regulation of carbohydrate metabolism and the major target tissues of CHH are the hepatopancreas, which plays an important role in energy storage for molting, and muscle, which is a major site of glycogen storage (Chan et al., 2003; Nagai et al., 2011; Webster et al., 2012). Because the hepatopancreas serves as the primary organ for the synthesis and storage of glycogen for the whole body, whereas muscle glycogen is used solely as a source of fuel by muscle itself, it was proposed that regulation of the activity of downstream target molecules may be distinctively different in hepatopancreas and muscle.

Changes in glycogen and total carbohydrate concentrations induced by stress are accompanied by an increased secretion of CHH (Basu and Kravitz, 2003; Kegel et al., 1989; Lorenzon et al., 2004, 2005; Reddy and Kishori, 2001). Since CHH is mainly synthesized in and secreted from the X-organ/sinus gland (XO/SG) complex in the eyestalk (Webster, 2015), eyestalk ablation is a common operation to study the function of CHH. After eyestalk ablation in the kuruma prawn *Marsupenaeus japonicus*, the transcript levels of glycogen phosphorylase and glycogen synthase decreased and increased, respectively, indicating that eyestalk ablation drives the metabolic state towards glycogen accumulation (Nagai et al., 2011). Furthermore, incubation of the hepatopancreas with CHH resulted in a decreased conversion rate of glucose into glycogen (Sedlmeier, 1987). These findings provide evidence that CHH is involved in glycogen metabolism in the hepatopancreas. Recently, Nagai and colleagues found that the *Bombyx mori* orphan neuropeptide G-protein-coupled receptors BNGR-A2 and BNGR-A34 act as ion transport peptide (ITP) receptors and show that BNGR-A24 is an ITP-like (ITPL) receptor (Nagai et al., 2014). However, in crustaceans, the CHH receptor in the hepatopancreas and downstream signal pathway that mediate these processes remain unidentified (Chung et al., 2010; Webster et al., 2012). It was demonstrated that the intracellular levels of hepatopancreatic cGMP, but not cAMP, decreased after eyestalk ablation (Nagai et al., 2011). An *in vitro* incubation study showed that the mode of action of CHHs involves cGMP as a second messenger and their binding caused a large amount of cGMP production, whereas 8-Br-cGMP mimics CHH-induced hyperglycemia (Chung and Webster, 2006). Therefore, protein kinase G, rather than protein kinase A, may be involved in CHH-induced kinase cascades in crustaceans. However, the identity of the molecule that interacts directly with CHH at the hepatopancreas membrane in crustaceans remains undetermined.

Our research here investigates the potential receptor of CHH, with an emphasis on membrane receptor-mediated signal transduction mechanism in the hepatopancreas. As a first step towards screening possible receptor candidates, we analyzed the transcriptome of the *Eriocheir sinensis* hepatopancreas revealed by digital gene expression (DGE). Among all the unigenes, we identified CHH

[1]Tianjin Key Laboratory of Animal and Plant Resistance, College of Life Science, Tianjin Normal University, Tianjin 300387, People's Republic of China. [2]Tianjin Center for Control and Prevention of Aquatic Animal Infectious Disease, Tianjin 300221, People's Republic of China.

*Author for correspondence (jinshsun@163.com)

Received 10 October 2015; Accepted 3 February 2016

Journal of Experimental Biology (2016) 219, 1259-1268 doi:10.1242/jeb.133181

binding protein (CHHBP) as the target. Here, we describe the binding affinity between CHH and CHHBP. We also show CHHBP sequence analysis, its expression pattern, localization in hepatopancreatic cells and the effect of RNAi-mediated knockdown of CHHBP.

MATERIALS AND METHODS

Animals and tissues

Chinese mitten crabs (*Eriocheir sinensis* Milne-Edwards 1853) were obtained from the Tianjin Aquaculture Disease Prevention and Treatment Center. Healthy crabs were acclimated for 2 weeks prior to the experiment and fed once every 2 days with fresh fish. Water temperature was maintained at 20±1°C, and a 12 h light:12 h dark photoperiod was used. Crabs were starved after eyestalk ablation in order to exclude the effects of diet on carbohydrate metabolism. Crabs were anesthetized on ice then killed and various tissues, including the hepatopancreas, muscle, heart, gill, gut, ganglia, ovary and testis were dissected out, frozen in liquid nitrogen and ground for total RNA or protein extraction. All animal studies were performed with the approval of Tianjin Normal University Animal Ethics Committee.

Total RNA isolation and cDNA synthesis

Total RNA from different tissues was extracted using TRIzol Reagent (Invitrogen) according to the manufacturer's instructions. The integrity of RNA was determined by agarose gel electrophoresis. The concentration of RNA was determined by measuring the absorbance at 260 nm in a spectrophotometer (Thermo Fisher Scientific). The total RNA was then reverse-transcribed into first-strand cDNA using M-MLV reverse transcriptase (Promega) and oligo-dT primer [5′-GGCCACGCGTCGACTAGTAC(T)16(A/C/G)-3′] according to the manufacturer's instructions.

Rapid amplification of cDNA ends (RACE)

A specific fragment of cDNA encoding *E. sinensis* CHH binding protein was obtained through transcriptome analysis, which includes the C-terminus of the ORF and part of the 3′-UTR. To obtain the N-terminal fragment of the ORF, 5′ rapid amplification of cDNA ends with gene-specific primers (5R1 and 5R2, Table 1) was performed using the GeneRacer kit (Invitrogen). The sequence of the *CHHBP* gene was imported into EditSeq of DNASTAR software and determined using Blastn and Blastx on the NCBI website. The nucleotide sequences of CHHBP-encoding cDNAs were submitted to GenBank under accession number KJ700937.

Expression and purification of the rCHH and rCHHBP

BL21(DE3) pLysS cells were transformed with the constructed plasmids encoding recombinant His-tagged CHH (rCHH) and CHHBP (rCHHBP). Cultures of the transformants grown in LB broth containing 50 μg ml^{-1} ampicillin and 50 μg ml^{-1} kanamycin, respectively, at 37°C were induced with 1 mmol l^{-1} IPTG at OD_{600}=0.6 for 6 h. Cultured cells were harvested by centrifugation at 4000 rpm and 4°C. Bacterial pellets were resuspended in fragmentation buffer (50 mmol l^{-1} Tris-HCl, 100 mmol l^{-1} NaCl, 2 mmol l^{-1} EDTA, 0.5% Triton X-100, 1 mg ml^{-1} lysozyme, pH 7.4). Sonicated lysates were cleared by centrifugation at 10,000 rpm, 4°C. Inclusion bodies were washed (washing buffer: 300 mmol l^{-1} KCl, 50 mmol l^{-1} KH_2PO_4, 5 mmol l^{-1} imidazole and 1 mol l^{-1} urea) three times, then dissolved in binding buffer (300 mmol l^{-1} KCl, 50 mmol l^{-1} KH_2PO_4, 5 mmol l^{-1} imidazole with 8 mol l^{-1} urea). rCHH and rCHHBP were purified through immobilized metal-affinity chromatography (IMAC) column (GE) and refolded by step-wise dialysis through 8.0, 6.0, 4.0, 3.0, 2.0, 1.0, 0.5 and 0 mol l^{-1} urea buffer (50 mmol l^{-1} Tris-HCl, 20 mmol l^{-1} NaCl, pH 7.8). The sequences of the purified proteins were analyzed and verified using mass spectrometry (data not shown).

Measurement of CHH and CHHBP binding affinity using biolayer interferometry

Binding kinetics and affinities between CHH and CHHBP were determined at 30°C in solid black 96-well plates (Greiner Bio-One, Baden-Württemberg, Germany) using an Octet Red96 (ForteBio, Menlo Park, CA, USA). Streptavidin-coated biosensors (SA biosensors, ForteBio) were equilibrated in physiological saline for crab (205.13 mmol l^{-1} NaCl, 5.37 mmol l^{-1} KCl, 13.51 mmol l^{-1} $CaCl_2$, 2.61 mmol l^{-1} $MgCl_2{\cdot}6H_2O$, 2.39 mmol l^{-1} $NaHCO_3$ and 13.93 mmol l^{-1} HEPES); this buffer was also used for washing, association and dissociation steps. The biosensors were then loaded with 10 μmol l^{-1} biotinylated rCHH, which was captured by biosensors during a 300 s incubation. Unbound rCHH was removed in a 60 s wash with physiological saline. Four decreasing concentrations (1.6-fold serial dilutions starting at 452 nmol l^{-1}) of rCHHBP as the analyte were equilibrated in the same buffer. Serial dilutions of rCHHBP were allowed to associate in physiological saline for 300 s and dissociation from rCHH was monitored for 600 s. To correct for non-specific binding of the protein to the biosensors, a parallel set of SA biosensors were loaded in saline buffer without CHHBP as a reference. The binding kinetics were processed and evaluated by ForteBio Data Analysis Software 7.0 using a 1:1 binding model to fit the curves.

Cells, transfection and confocal microscopy

Sf9 cells (ATCC number CRL-1711) were plated at a density of $5{\times}10^5$ cells cm^{-2} in SFM medium (Invitrogen) supplemented penicillin (100 μg ml^{-1}) and streptomycin (100 μg ml^{-1}). pIZ-

Table 1. Primers used in this study

Primer	Length (bp)	Position	Direction	Sequence (5′-3′)
5R1	27	837–863	R	CTCCACCACCTTCGTCTCCATCACTTC
5R2	27	760–786	R	CGGTTTCTGCTTGCTTAGCCCGAACCT
QF	21	1224–1244	F	GTGTCCTCAGGTGACTCTCCT
QR	21	1354–1374	R	GCTTTGTGTTGTTCTTCGTTC
ActinF	22	208–229	F	GGTTGCCGCCCTGGTTGTGGAC
ActinR	19	429–447	R	TTCTCCATGTCGTCCCAGT
GiF	31	125-147	F	GCTCTAGAAGCTTACCCTTAAATTTATTTGC
GiR	29	464–483	R	CCGGAATTCTCCATTCTTTTGTTTGTCTG
iF	28	739–758	F	GCTCTAGAAGAAAGCCACTTATGACCAG
iR	27	1388–1405	R	CCGGAATTCTGTGCCTTCCCTTAGGAT

The underlined regions represent the recognition sequences of the restriction endonucleases. ActinF and ActinR were designed according to cDNA sequences in GenBank (accession no. HM053699.1). F, forward; R, reverse.

Journal of Experimental Biology

Journal of Experimental Biology (2016) 219, 1259-1268 doi:10.1242/jeb.133181

mCherry-CHHBP was derived from pmCherry-C1 vector and an insect vector pIZ/V5-His (Invitrogen). Cloned mCherry and CHHBP fragments were inserted into the multiple cloning sites of pIZ/V5-His vector. The resulting reporter plasmid pIZ-cherry-CHHBP was purified from *Escherichia coli* with a Qiagen plasmid midi kit. Sf9 cells were transfected with this plasmid using X-tremeGENE HP DNA transfection reagent (Roche) according to the manufacturer's instructions. After transfection, cells were cultured for 36 h to express the foreign protein. Then, to detect the interaction between CHH and CHHBP, cells were incubated for 1 h with 200 nmol l^{-1} DyLight-488-coupled-rCHH and -rTHRB (thyroid hormone receptor, as a control; DyLight 488 NHS Ester, 46403, Thermo) respectively, in serum- and glucose-free medium. Cells were then processed for confocal microscopy on a Nikon Eclipse 90i. Brightness and contrast of images were adjusted in Adobe Photoshop (Adobe Systems).

Western blot analysis

Tissue homogenates (after extracting for cellular protein) were boiled in loading buffer and separated on 12.5% SDS-polyacrylamide gels. Protein was transferred onto PVDF membranes (Millipore, Billerica, MA) using standard methods. Membranes were blocked overnight at 4°C in 5% skimmed milk and probed for 3 h at room temperature with the following primary antibodies: anti-CHHBP raised in rabbits (1:1500; Beijing Protein Innovation Co., cat. no. 73228) and anti-tubulin (1:1000; Beyotime Institute of Biotechnology, cat. no. AT819). After washing twice with 20 mmol l^{-1} Tris-HCl (pH 8.2), 150 mmol l^{-1} NaCl, 0.05% Tween 20 (TBST) and blocking using 2.5% skimmed milk, the membranes were incubated with either anti-rabbit or anti-mouse HRP-conjugated secondary antibody for 2 h. After washing with TBST, membranes were processed for detection of antibody binding using ECL Plus (Beyotime Institute of Biotechnology, Jiangsu, China) and visualized with Eastman Kodak film according to the manufacturer's instructions.

Immunohistochemistry

Fresh hepatopancreas samples were fixed overnight at room temperature in 4% paraformaldehyde. After dehydration through a graded series of ethanol solutions, the tissue was embedded in hard paraffin and then cut into sections (5 µm thick) using a microtome (Leica RM2016). Consecutive sections were immunostained according to a standard protocol. Briefly, sections were incubated overnight at 4°C either with or without (negative control) the anti-CHHBP antibody (1:100; Beijing Protein Innovation Co., Beijing, China), followed by incubation with a secondary goat anti-rabbit IgG antibody (Santa Cruz). Binding of the secondary antibody was detected using diaminobenzidine (DAB). Sections were counterstained with hematoxylin and viewed under a light microscope. To determine glycogen distribution within the crab hepatopancreas, 3-µm-thick sections were stained by periodic acid-Schiff (PAS) staining using standard methods.

Quantitative PCR

Equal amounts of RNA from the hepatopancreas at 12, 24, 36, 48, 72, 96 h after the eyestalk ablation were submitted to quantitative RT-PCR. Total RNA was reverse transcribed into first strand cDNA in a 20 µl final reaction mixture using M-MLV reverse transcriptase (Promega). Quantitative PCR was performed in a 25 µl reaction volume containing cDNA sample derived from 50 ng of total RNA and two primer sets: one for *CHHBP* and the other for β-actin, which was used as a control. The PCR was 33 cycles: denaturing at 94°C for 30 s, annealing at 56°C for 30 s and extension at 72°C for 30 s. PCR reactions were performed using Ex *Taq* DNA polymerase (TaKaRa) and an IQ5 real-time PCR detection system (Bio-Rad) according to the manufacturer's protocol.

Synthesis and injection of double-stranded RNA

Reconstructed plasmids that contained two inverted T7 promoter sites flanking the cloning region were obtained (named as pET-T7) as described previously (Dai et al., 2008). Next, a 667 bp fragment containing part of the coding region of the *CHHBP* gene was amplified by PCR with primers iF and iR (Table 1). This amplified fragment was excised using *Xba*I and *Eco*RI and then subcloned into pET-T7. For the negative control, a 359 bp GFP cDNA fragment was amplified from pcDNA3.1/CT-GFP-TOPO plasmid (Invitrogen) using primers GiF and GiR (Table 1) and subcloned into pET-T7 at the same restriction sites. After transformation into *E. coli* DH5α, inserted nucleotide sequences of the recombinant plasmids were confirmed by DNA sequencing. Recombinant plasmids were then transformed into *E. coli* HT115 and the dsRNAs purified as described by Yodmuang et al. (2006).

Blood glucose measurement

Hemolymph samples for glucose level estimation were extracted from the base of a crab walking leg with a hypodermic syringe and immediately mixed with an equal volume of anticoagulant (0.3 mol l^{-1} NaCl, 20 mmol l^{-1} trisodium citrate, 26 mmol l^{-1} citric acid, 1 mmol l^{-1} EDTA). The blood glucose level was measured using a glucose assay kit (Rongsheng Biotech Co., Shanghai, China). To detect the glucose level on the effect of rCHH, crabs (30 g±10 g) were injected with 1.5 µg rCHH each. Hemolymph samples were extracted at 0 h, 1 h, 2 h, 4 h and 6 h after injection.

2-NBDG transport assay

Sf9 cells were transfected with the pIZ-cherry-CHHBP vector or pIZ-cherry vector as a control. 36 h after transfection, cells were grown in glucose-free medium for 30 min and then incubated with the same medium containing 80 µmol l^{-1} 2-NBDG (N13195, Invitrogen) at 27°C for 60 min. The uptake reaction was stopped by washing the cells three times with 1× phosphate-buffered saline, pH 7.2. To assess the influence of CHH, the medium was then replaced with glucose-free medium containing 80 µmol l^{-1} rCHH. Another group of cells transfected with pIZ-cherry-CHHBP vector was incubated without rCHH to act as a negative control. Live cells were visualized with Nikon Eclipse 90i confocal microscope under a 100× oil immersion objective lens.

RESULTS

Cloning and sequence analysis of CHHBP

To identify the downstream effector molecule in glucose metabolism regulated by CHH, Illumina RNA-Seq and DGE analysis were performed. The hepatopancreas and muscle are the major target tissues of CHH and considering the more important role of the hepatopancreas in metabolism, we ultimately selected the hepatopancreas for analysis. The transcriptome of the *E. sinensis* hepatopancreas revealed by DGE analysis identified 1416 unigenes that were significantly differentially expressed following eyestalk ablation, which indicated that they were likely to be involved in metabolism. All of the identified unigenes were aligned against the Nt, Nr and Swiss-Prot databases using BlastN and BlastX searches with an E-value less than 10^{-5}. In addition, to identify the biological pathways necessary for regulating metabolism in *E. sinensis*, the

Journal of Experimental Biology (2016) 219, 1259-1268 doi:10.1242/jeb.133181

unigenes were also matched to the reference canonical pathways in KEGG. During screening, the unigene annotated as flotillin, which was assigned to the insulin signaling pathway, attracted our attention. This gene in *E. sinensis* (identified as *CHHBP* subsequently) was upregulated 2.8-fold after removal of the eyestalk. Sequence information provided by transcriptome analysis revealed a *CHHBP* cDNA of 819 bp, including the termination codon and part of the 3′-UTR, but not the initiation codon. 5′ RACE was performed to obtain the full-length *CHHBP* open reading frame (ORF). The resulting cDNA (1438 bp) encoded a full-length ORF 1281 bp in length, corresponding to 426 amino acid residues with a predicted molecular mass of 47 kDa. The deduced amino acid sequence was 48% identical to that of flotillin-1 from *Homo sapiens* (GenBank accession no. NM_005803). Sequence blast and alignment showed that *CHHBP* was composed of one SPFH (stomatin/prohibitin/flotillin/HflK/C) domain from the 6th to the 188th amino acid at the N-terminus and a typical flotillin domain at the C-terminus.

As flotillin family members usually contain characteristic residues and potential phosphorylation sites (Morrow et al., 2002), motif scans were performed using the Hits homepage (http://hits.isb-sib.ch) to determine whether CHHBP also possessed these specific residues. Fig. 1 shows the amino acid sequence of CHHBP aligned with that of human flotillin-1. In addition to the classic SPFH domain and flotillin domain, CHHBP also contained potential casein kinase II phosphorylation sites and potential protein kinase C phosphorylation sites. As flotillin family members have a well-defined hydrophobic putative intramembrane domain, hydropathy analysis of the CHHBP protein was performed using the Tmpred program (http://www.ch.embnet.org/software/TMPRED_form.html). The results suggested that one hydrophobic domain (residues 12–39) might function as a potential transmembrane domain. This gene shared no apparent homology with any other known genes or proteins in the DDBJ/EMBL/GenBank database.

Although CHHBP exhibited some properties in common with human flotillin-1, an interesting difference drew our attention: two potential cAMP- and cGMP-dependent protein kinase phosphorylation sites were observed in the region from residues 94–97 and 222–225 in the CHHBP protein. Since CHH functions in Y-organ through signaling pathways that converge at cGMP (Chung and Webster, 2003; Webster et al., 2012), the presence of these sites allowed us to make predictions about the signal processor and transmitter roles of CHHBP.

CHHBP interacts with CHH

To detect whether this receptor candidate was able to interact with CHH, we next investigated the direct binding of recombinant CHHBP to CHH. First, rCHH and rCHHBP were obtained using a prokaryotic expression system and purified (Fig. 2A,B). Then, binding affinity was tested using a novel biolayer interferometry (BLI) assay. Based on interferometry, BLI is a label-free method to calculate interactions of soluble analytes with a sensor surface, onto which the corresponding interaction biomacromolecule is immobilized. In this study, a sensorgram of rCHH on streptavidin-coated biosensors binding to different concentrations of CHHBP was investigated. The results of BLI confirmed that CHHBP binds to CHH (Fig. 2C). Different concentrations of the analyte were measured to evaluate the binding kinetics and affinities. The K_D was measured as 1.83×10^{-9} mol l^{-1} and the R^2 value was 0.97. These results confirmed that CHH interacts with CHHBP in a specific and strong manner.

To evaluate the *in vitro* interaction between CHH and CHHBP, we visualized the colocalization of CHH and CHHBP on the membrane of sf9 cells by confocal microscopy (Fig. 3). CHHBP localized to the membrane (Fig. 3, top row). Dylight-488-labeled CHH added to the culture medium colocalized with CHHBP at the cell membrane (Fig. 3, top right panel, yellow). However, Dylight-488-labeled THRB, which was used as a negative control, showed no overlap with CHHBP but localized to other regions of the cell membrane (Fig. 3, bottom row, arrows). Such subcellular localization suggested again that CHHBP strongly interacts with CHH.

Tissue distribution and cellular localization of CHHBP proteins

To determine the tissue distribution of CHHBP, immunoblotting was performed on crude protein extracted from the hepatopancreas, muscle, heart, gill, gut, ganglia, ovary and testis. Under different development times, the western blot results showed that, at the protein level, CHHBP is detected in hepatopancreas, muscle, heart,

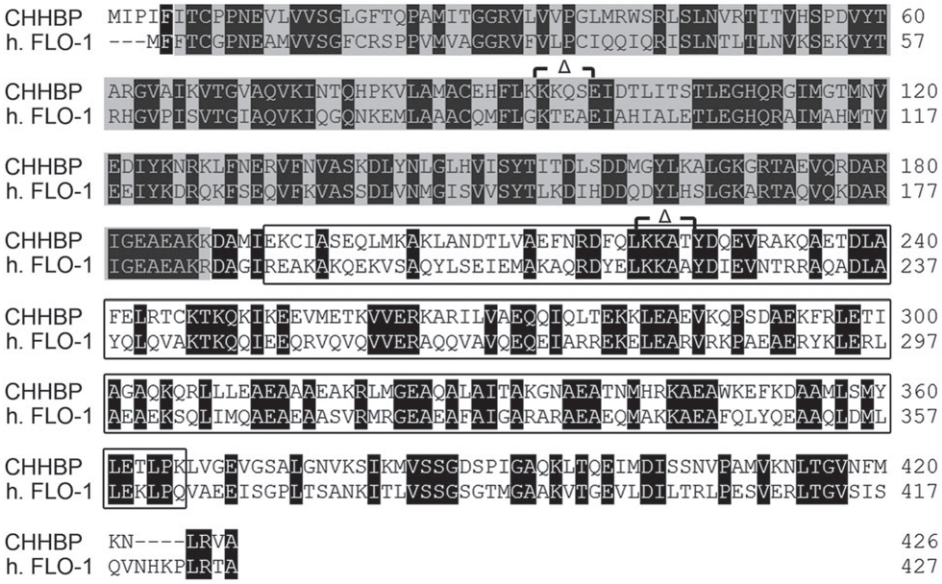

Fig. 1. Amino acid sequence alignment between *CHHBP* and human flotillin 1 (*FLOT1*). The SPFH domain is shaded in gray and the flotillin domain is boxed. The potential sites for phosphorylation by cAMP- and cGMP-dependent protein kinases (Δ) in *CHHBP* are indicated.

Journal of Experimental Biology (2016) 219, 1259-1268 doi:10.1242/jeb.133181

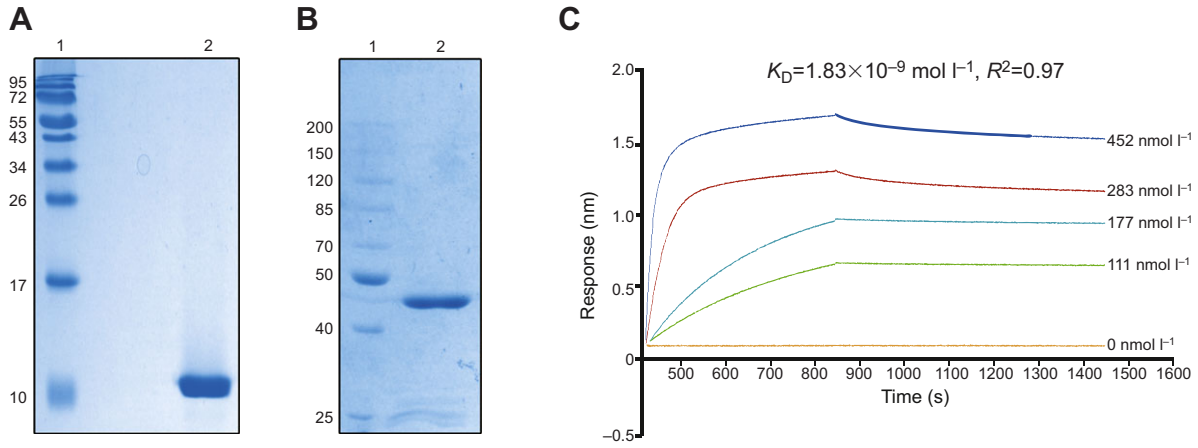

Fig. 2. Interaction of CHH with CHHBP. (A) Purified recombinant CHH (lane 2) and Esflol (B, lane 2) were assessed by SDS-PAGE, exhibiting a molecular mass near 11 kDa and 49 kDa, respectively. (C) Binding kinetic analysis of CHHBP to CHH using biolayer interferometry. Sensorgram of CHH on streptavidin-coated biosensors binding to different concentrations of CHHBP is shown. The light orange line indicates the blank reference. The binding affinity parameter K_D was calculated and is shown above the binding curve. R^2 is the coefficient of determination for estimating the goodness of a curve fit reported by ForteBio Data Analysis Software 7.0.

gut and gill, but not in the ganglia, ovary or testis (Fig. 4A). Additionally, CHHBP was strikingly enriched in the hepatopancreas compared with other tissues. Since the hepatopancreas and heart are important tissues for glycogen storage and decomposition, and because the gut acts as the main site of digestion and absorption of nutrients, including sugar, this finding supports the hypothesis that CHHBP is involved in glucose metabolism. Furthermore, as mentioned above, the hepatopancreas and muscle are the major target organs of CHH in crustaceans. The predominant expression of CHHBP in the hepatopancreas suggests that it plays an important role in the regulation of CHH in cellular metabolism. Taken together, these results indicate that CHHBP serves as the messenger molecule that transmits the CHH signal from the outside to the inside of the cell.

To further characterize the expression of CHHBP in crab hepatopancreatic cells, tissue sections from the hepatopancreas were examined by immunohistochemistry (Fig. 4B). CHHBP was found to be localized to the cell membrane in hepatopancreatic cells (as indicated by the arrows in Fig. 4B). No signal was detected in the negative control (data not shown).

Temporal expression profiles of CHHBP after eyestalk ablation

As it is known that CHH is produced by the X-organ sinus gland (XO-SG) complex, we removed the neuroendocrine system by cutting the eyestalk, thus effectively severing the relationship between endogenous CHH and CHHBP. The mRNA expression levels of *CHHBP* in intact and eyestalk-ablated crabs were analyzed by quantitative PCR at 12, 24, 36, 48, 72 and 96 h after eyestalk ablation (Fig. 5). Interestingly, compared with the control group, expression of *CHHBP* mRNA in the eyestalk-ablated crabs decreased at 12 and 24 h, then increased and peaked at 36 h, followed by a decrease. In addition, although the expression levels of *CHHBP* mRNA decreased after 36 h, it remained upregulated ~2-fold compared with the control group. The changes in *CHHBP* transcription levels coordinated with elimination of CHH. Considering that the samples used for transcriptome analysis were taken from the hepatopancreas of crabs with or without eyestalk ablation exactly 48 h after treatment, this finding confirmed that CHHBP is involved in the signaling cascades induced by CHH. When considered with our finding that CHHBP localizes to the

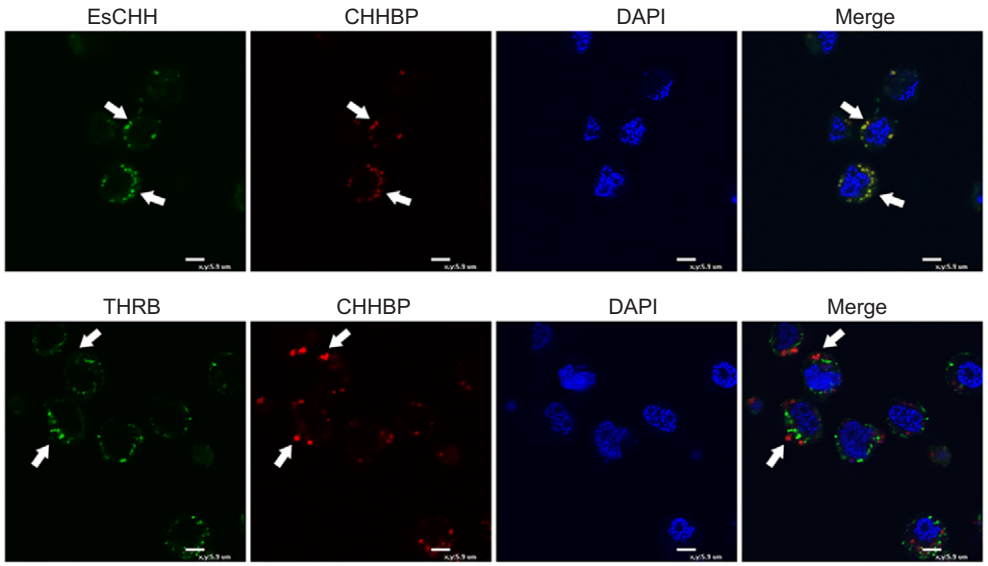

Fig. 3. Colocalization of CHH and CHHBP in sf9 cells. pIZ-cherry-CHHBP vector was transfected and expressed in sf9 cells, shown red in confocal microscopy. As seen in the second panels of both rows, CHHBP is localized in the cell membrane. Dylight-488-labeled CHH (top row, green) added to the culture medium colocalized with CHHBP (top row, red) at the cell membrane (top row, arrows), suggesting that CHHBP could interact with CHH. Dylight-488-labeled THRB showed no overlap with CHHBP (bottom row) but localized to other regions of the cell membrane (bottom row, arrows). Scale bars: 5.9 μm.

Journal of Experimental Biology (2016) 219, 1259-1268 doi:10.1242/jeb.133181

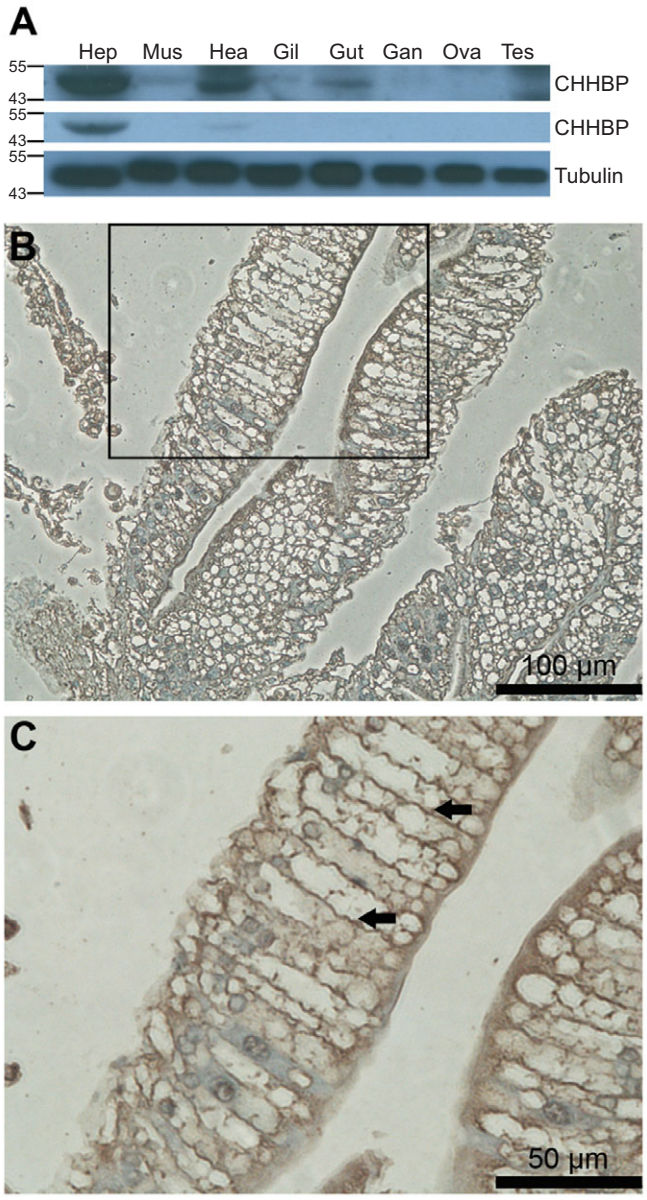

Fig. 4. Localization of CHHBP in crab. (A) Western blot analysis of tissue-specific expression of CHHBP. Total protein (100 μg) from crab tissues was hybridized with anti-CHHBP antibody. CHHBP expression was clearly detected in the hepatopancreas and heart, and weakly in the muscle, gut and gill. Tubulin levels were also probed as a measure of protein loading. Hep, hepatopancreas; Mus, muscle; Hea, heart; Gil, gill; Gan, ganglia; Ova, ovary; Tes, testis. (B,C) Localization of CHHBP in the hepatopancreas. Immunoperoxidase staining of a representative paraffin-embedded hepatopancreas sample with DAB shows staining of the cell membrane, with the cytoplasm remaining negative. Arrows in C indicate positive staining on the membrane of the hepatic cells.

membrane, we had reasonable grounds for believing it is a signal messenger that links extracellular hormones to intracellular metabolic responses.

Depletion of CHHBP leads to a decreased blood glucose level that is not rescued by CHH

dsRNA designed based on the *CHHBP* and *GFP* cDNA sequences were injected into the body cavity of juvenile crabs. RNAi efficiency was evaluated on the second day after injection. As

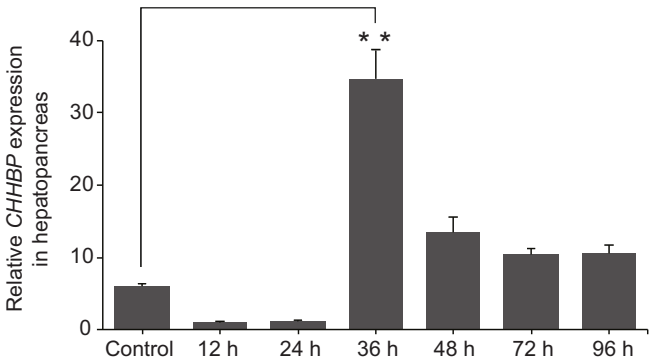

Fig. 5. Time-course of transcript levels of *CHHBP* in the hepatopancreas of crabs after eyestalk ablation. *CHHBP* transcript expression level at 12, 24, 36, 48, 72 and 96 h after eyestalk ablation determined by quantitative PCR. β-actin was used as an internal control. The primer sets used are listed in Table 1. Results shown represent the means±s.e. (n=3). $^{**}P$<0.01 using one-way ANOVA followed by Duncan's analysis using SPSS software version 11.0.

shown in Fig. 6A, injection of 10 μg of dsRNA per crab almost completely knocked down expression of endogenous *CHHBP* compared with the control group.

To address the function of CHHBP in glucose regulation, blood glucose levels were examined using a glucose assay kit (Fig. 6B). As expected, the test group displayed much lower levels of blood glucose than the control group injected with *GFP* dsRNA, reflecting a defect in glucose regulation resulting from knockdown of CHHBP. Meanwhile, to evaluate the relationship between CHHBP and CHH, the blood glucose levels of crabs subjected to eyestalk ablation were also measured. The results showed that 2 days after the removal of CHH via eyestalk ablation, blood glucose levels were markedly reduced compared with the group without any surgical intervention. In addition, we found that the reduction in blood glucose levels induced by eyestalk ablation reached the same level as that in the group treated with *CHHBP* dsRNA.

To verify the role of CHHBP in the regulation of glucose levels, we injected rCHH (Fig. 2A) into crabs which were injected with *GFP* dsRNA (control) and *CHHBP* dsRNA (test) in advance, respectively. Results showed that in the control group, rCHH led to a gradually increased glucose level from 0 h to 2 h after the injection, followed by a gradually reduced glucose level. However, the already reduced glucose level induced by *CHHBP* RNAi could not be rescued by injection of rCHH (Fig. 6C). These results strongly support the hypothesis that CHHBP acts as the signal receptor or processor of CHH activity in the regulation of cellular glucose metabolism.

Histological studies

To further define the role of CHHBP in metabolism, we performed RNAi-mediated knockdown of CHHBP in the hepatopancreas, the main organ for synthesis and storage of glycogen for the whole body. Cells in the hepatopancreas of *E. sinensis* juveniles treated with *GFP* RNAi (control) exhibited normal cellular morphology and arrangement of fibrillar cells and resorptive cells (Fig. 7A, black arrow). PAS reaction revealed that the glycogen was localized near the cell membrane on the side of the hepatic duct (Fig. 7A, black arrowhead). However, hepatic cells in the *CHHBP* RNAi groups appeared to be damaged in some way (Fig. 7B, white arrow), or to contain large vacuoles (Fig. 7C, white arrow). Cells in sections from the test group contained much more stored glycogen than those from

Journal of Experimental Biology (2016) 219, 1259-1268 doi:10.1242/jeb.133181

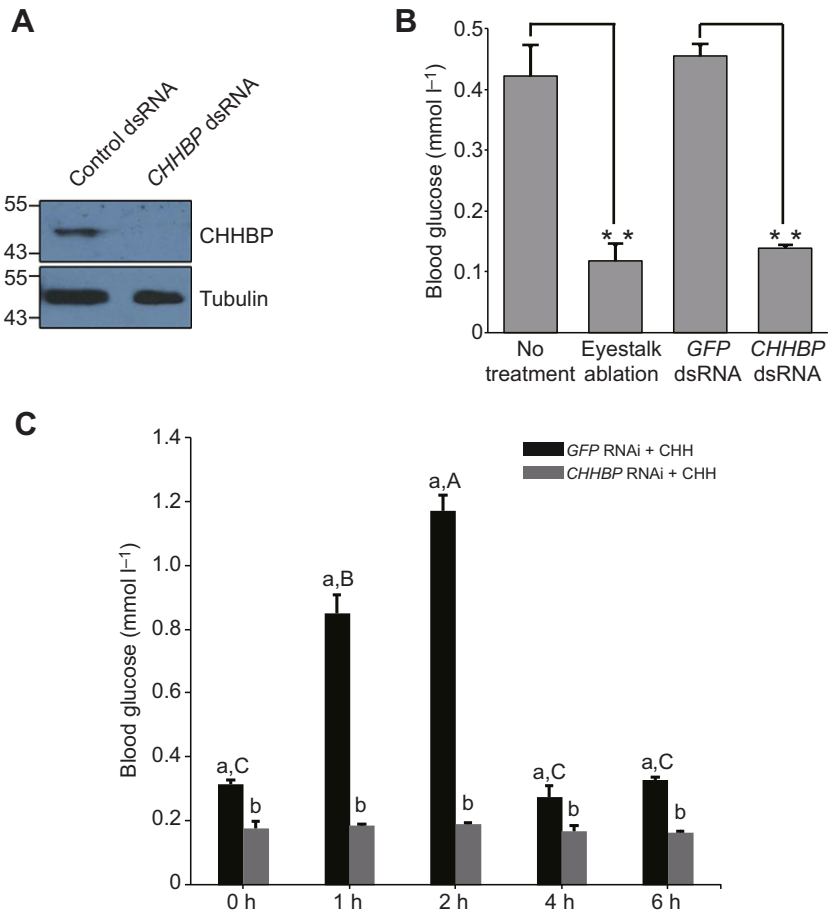

Fig. 6. Gene knockdown of *CHHBP* by RNAi in the crab. (A) Relative expression levels of *CHHBP* in the control (*GFP* RNAi) and *CHHBP* RNAi groups determined by immunoblotting. (B) After successful knockdown of CHHBP, the test group exhibited markedly lower blood glucose concentrations than the control group. Eyestalk ablation also induced lower blood glucose concentrations compared with the untreated group. Results shown represent means±s.e. (n=3). $^{**}P$<0.01 using one-way ANOVA followed by Duncan's analysis using SPSS software version 11.0. (C) Changes in glucose level in control (black bars) and *CHHBP* RNAi group (gray bars) after injection of rCHH. Values are presented as means±s.d. (n=3). Data labeled with different letters indicate a significant difference (P<0.05) among treatments.

the control group, and the glycogen showed a scattered (Fig. 7B, white arrowhead) or aggregated morphology (Fig. 7C, white arrowhead); these morphological findings are very similar to those observed in mammals with glycogen storage disease. The abnormal and massive glycogen deposition in hepatic cells suggests that knockdown of CHHBP disrupts CHH signaling during glucose metabolism and confirms that CHHBP plays an important role in this signaling cascade.

2-NBDG can be transported from the inside to the outside of the cell under combined action of CHH and CHHBP

Given that CHH was able to induce the increase in blood glucose and that CHHBP colocalized with CHH at the cell membrane, we examined whether CHHBP was involved in transport of 2-NBDG. First, cells transfected with plasmids encoding mCherry-CHHBP protein were treated with 2-NBDG. Following the 2-NBDG treatment, cells were divided into two groups: a control group of cells was incubated with glucose-free medium and test group was incubated with glucose-free medium containing rCHH. 2-NBDG fluorescence was located inside the cells in the control group (Fig. 8, first row). By contrast, most fluorescence signals in the test group disappeared from the inner cell but residual signals overlapped with CHHBP at the membrane (Fig. 8, second row). Thus, CHH was able to drive 2-NBDG, the glucose analog, to transport from the inner cell to the outside. Furthermore, to confirm that CHHBP is involved in the regulation of glucose transport via CHH, sf9 cells transfected

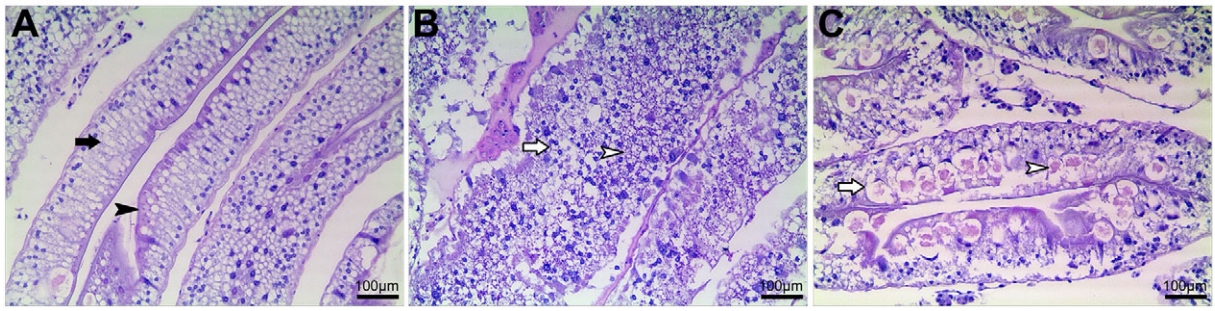

Fig. 7. Periodic acid-Schiff (PAS) staining of crab hepatopancreas after RNAi-mediated knockdown of *CHHBP*. Low-power magnification of RNAi-mediated knockdown of *GFP* (A) and *CHHBP* (B,C). Successful knockdown of CHHBP resulted in disrupted morphology (B) or vacuole formation (C) in hepatopancreatic cells (white arrows); however, this was not observed in the control group (A, black arrow). Glycogen stored in hepatic cells in the test group appeared scattered (B, white arrowhead) or aggregated (C, white arrowhead), whereas in the control group, the glycogen was orderly located on one side of the cells (A, black arrowhead).

Journal of Experimental Biology (2016) 219, 1259-1268 doi:10.1242/jeb.133181

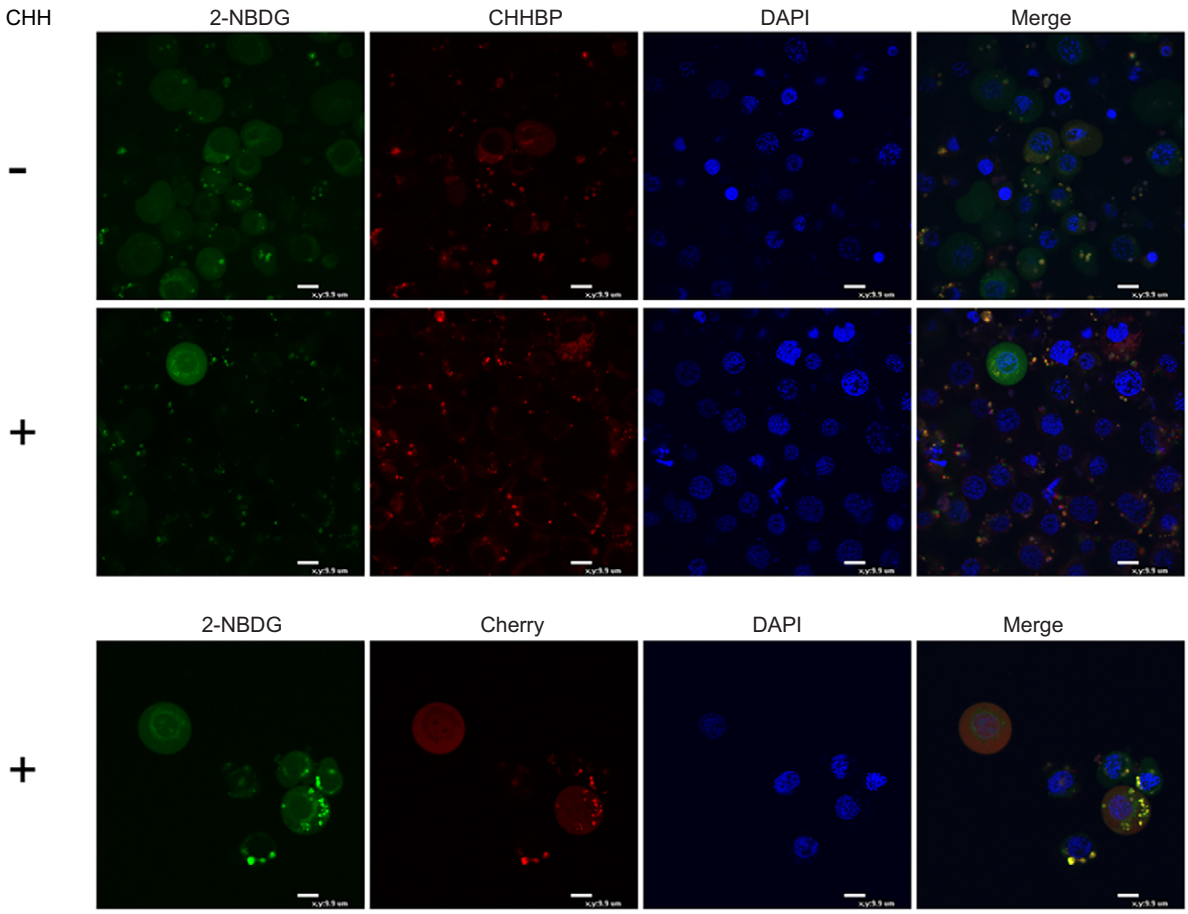

Fig. 8. 2-NBDG is transported out of cells under the combined action of CHH and CHHBP. Sf9 cells expressing mCherry-CHHBP were first grown in glucose-free medium and shifted to the same medium containing 80 μmol l^{-1} 2-NBDG and incubated for 60 min. The uptake reaction was stopped by washing with PBS followed by rCHH treatment (second row) or not stopped (top row). 2-NBDG fluorescence is located inside the cells (top row). By contrast, most of the fluorescence signal disappeared from inside the cell upon stimulation with rCHH, suggesting that CHH was able to drive 2-NBDG to transport from the inner cell to the outside. Residual signals overlapped with CHHBP at the membrane (second row). In addition, cells expressing mCherry alone (as a control) were also treated with 2-NBDG and subsequently, rCHH (bottom row). Unlike the results observed in cells expressing CHHBP, 2-NBDG was not transported but remained inside the cell, indicating that in the presence of CHH, CHHBP provides indispensable assistance for transport of 2-NBDG. Scale bars: 9.9 μm.

with plasmids encoding mCherry protein were also treated with 2-NBDG and subsequently, rCHH. Unlike in cells expressing CHHBP, 2-NBDG was not transported, but remained inside the cells expressing mCherry. Therefore, in the presence of CHH, CHHBP was essential for 2-NBDG transport, consistent with the above finding that CHHBP acts as the receptor for CHH.

DISCUSSION

Physiological processes are regulated by various neuropeptides that coordinate the activity of organ systems. In arthropods, most neuropeptides function through G-protein-coupled receptors and involve cyclic nucleotides (cAMP and cGMP) or Ca^{2+} in target tissues (De Loof, 2008; Hauser et al., 2006, 2008; Huang et al., 2008; Žitňan et al., 2007). In decapod crustaceans, MIH and CHH inhibit molting by activating signaling pathways that increase cAMP and cGMP in response to stress or changing environmental conditions. Previous studies indicate that crab Y-organ membranes have distinct receptors for MIH and CHH (Chung and Webster, 2003). The CHH receptor appears to be a membrane guanylyl cyclase (Chung and Webster, 2006; Webster et al., 2012). However, CHH is 10- to 20-fold less effective than MIH at inhibiting ecdysteroidogenesis (Chung and Webster, 2003), suggesting that its main function is controlling glucose metabolism in crustacean tissues (Sefiani et al., 1996; Yasuda et al., 1994). The main target tissues of CHH in regulation of glucose metabolism are the hepatopancreas and muscle. We found that CHHBP was enriched in the hepatopancreas and heart, it was also detected in muscle, gut and gill (with much less amount), but not in ganglia, ovary or testis (Fig. 4A). Hepatopancreas and heart are important tissues for glycogen storage and decomposition, and the gut acts as the main site of digestion and absorption of nutrients, including sugar. More importantly, the hepatopancreas, heart, muscle, gut and gill have all been shown to possess specific binding sites for CHH family peptides (Chung et al., 2010). It is probably not a coincidence that the tissues which express CHHBP in *Eriocheir sinensis* are the same as the main target tissues of CHH. Furthermore, in *Bombyx mori*, expression of the putative ITP receptors BNGR-A2 and BNGR-A34 was restricted to some, but not all of these tissues (Nagai et al., 2014), which is somewhat comparable to the expression profile of *CHHBP*.

Although many studies have demonstrated multiple target tissues of CHH, the CHH receptor and signal transduction pathways that are activated by CHH in these tissues remain unidentified (Chung et al., 2010; Webster et al., 2012). Inspiringly, Nagai et al. (2014) describe

Journal of Experimental Biology (2016) 219, 1259-1268 doi:10.1242/jeb.133181

the identification of several GPCRs as putative ITP receptors. Since ITP and CHH belong to the same superfamily of CHH and are both categorized as type I neuropeptides, this finding gives us important information about the CHH membrane receptor in crustacea. However, putting aside the similarities between ITP and CHH, we also should note their differences and uniqueness. At the gene level, since there are many CHH isoforms and variants even in one and the same species, it is not hard to imagine that sequence differences exist between insect ITPs and aquatic crustacea CHHs. However, studies on the biochemical identity of ITPs in insects are limited. To date, ITPs are found to mainly regulate energy metabolism, molting and reproduction by modulating homeostasis mechanisms, whereas CHHs chiefly affect energy balance by regulating glucose metabolism. Many details of how CHH family members exert their pleiotropic effect in downstream signaling pathways remain to be elucidated. So far, the transport-stimulating effect of ITP is assumed to be mediated by cAMP, whereas CHH is considered to perform its function through recruitment of cGMP. Above all, the differences between ITPs and CHHs and the lack of information of their regulatory mechanisms gave us an opportunity to investigate potential candidates for the membrane receptor of CHH. Here, we aimed to identify the downstream effector molecule in the cascade of glucose metabolism regulated by CHH using Illumina RNA-Seq and DGE analysis. Among the unigenes that were significantly differentially expressed following eyestalk ablation, we selected a flotillin-like protein (which we subsequently named CHHBP) for analysis based on its annotated function in glucose metabolism in humans and the finding that *CHHBP* mRNA levels were upregulated 2.8-fold after removal of the eyestalk. These results were a strong indication that CHHBP is involved in glucose metabolism in the hepatopancreas of *E. sinensis*.

We cloned the cDNA sequence encoding *CHHBP* and compared its amino acid sequence with that of human flotillin-1. We found that the N-terminus of the CHHBP protein contains an SPFH domain in the region spanning residues 6–188. The SPFH domain exists in several eukaryotic and prokaryotic membrane proteins, such as prohibitin, stomatin and podocin, which have numerous and diverse functions (Tavernarakis et al., 1999). However, CHHBP differs from other SPFH family members in that it also has a well-defined hydrophobic putative intramembrane domain, suggesting that CHHBP functions as a transmembrane protein. This conclusion was supported by the results of immunohistochemical analysis of hepatopancreas sections (Fig. 4B). Interestingly, sequence analysis also revealed that CHHBP contains two potential cAMP- and cGMP-dependent protein kinase phosphorylation sites (Fig. 1). Because in crustaceans, intracellular levels of cGMP or cAMP decrease in the hepatopancreas after eyestalk ablation (Nagai et al., 2011), the presence of these cAMP- and cGMP-dependent protein kinase phosphorylation sites suggests that CHHBP is involved in signaling pathways that interact with cAMP/cGMP messengers. Together, these results provide evidence that CHHBP is part of the signaling pathway regulated by CHH.

Our K_D value for the binding of recombinant CHHBP to CHH was measured as 1.83×10^{-9} mol l^{-1}. Previous results indicated a K_D value of 1.68 (±0.34)$\times10^{-10}$ mol l^{-1} for the hepatopancreas in *Callinectes sapidus* (Chung et al., 2010). However, the binding assay carried out by Chung and colleagues was based on a homologous radioligand binding experiment. CHH was expressed in a prokaryotic system, iodinated and incubated with the membrane preparations from various tissues. By contrast, BLI is a label-free method used to calculate the interactions between two soluble analytes with a sensor surface, onto which the corresponding interaction macromolecule is immobilized. Even though both proteins tested in our BLI experiments were also purified from prokaryotic systems, differences between our methods and experimental design and those of Chung et al. (2010) could be the source of the differences in the two K_D values.

Flotillins are evolutionarily conserved and ubiquitously expressed. Although their exact functions remain controversial, they are considered to be active signaling partners that take part in various vital cell processes (Zhao et al., 2011). Previous research in humans showed that GLUT4 colocalizes with flotillin-1 in perinuclear regions in skeletal muscle cells under basal conditions. Following stimulation with insulin, GLUT4 moves to the sarcolemma, where uptake of glucose occurs. When flotillin-1-based domains are inhibited by treatment with a cholesterol-sequestering agent, GLUT4 translocation and glucose uptake fail to occur following insulin stimulation (Fecchi et al., 2006). Nevertheless, there have been few reports of regulation of flotillin by hyperglycemic hormones. In crustaceans, the membrane molecule that directly interacts with CHH and the downstream signal transduction pathway is still unknown (Chung et al., 2010; Webster et al., 2012). In our study, CHHBP can be induced by lack of CHH. The half-life of CHH in the blood is only ∼10 min. However, CHH is secreted when the body needs it to increase the blood glucose level. Therefore, CHH functions intermittently. After eyestalk removal, the lack of CHH causes a stressful situation, which forces increased expression of its receptor to capture any remaining CHH. Moreover, knockdown of CHHBP activity in the crab using dsRNA reduced blood glucose levels to the same degree as eyestalk ablation. This reduction could not be rescued by injection of rCHH. Consistent with the findings described above, these results suggest that CHHBP is involved in the signaling pathway that mediates glucose metabolism regulated by CHH. Furthermore, they strongly suggest that CHHBP acts as the CHH receptor in the hepatopancreas.

Treatment with *CHHBP* RNAi induced disrupted morphology and vacuolation of hepatopancreatic cells. In previous studies, hypertrophy of hepatic cells was reported in response to increased levels of gelatinized carbohydrate in the feed of *Labeo rohita* fry (Mohapatra et al., 2003) and *Acipenser baeri*. In addition, numerous studies have reported vacuolation in hepatic cells in glycogen storage disease in mammals (Brix et al., 1995; Kishnani et al., 2001). Based on this and the important role of CHHBP in glucose metabolism, the vacuolation of hepatopancreatic cells observed in our RNAi experiment may be the result of glycogen deposition. More importantly, previous studies showed that after eyestalk ablation in the kuruma prawn, *Marsupenaeus japonicus*, transcript levels of glycogen phosphorylase and glycogen synthase remarkably decreased and increased, respectively, indicating that decreased levels of CHH drive the metabolic state towards glycogen accumulation (Nagai et al., 2011). Based on the above findings, CHHBP appears to be involved in glucose metabolism regulated by CHH in *E. sinensis*.

Following BLI binding analysis and colocalization of CHH and CHHBP in cells, we determined the bioactivity of CHHBP in glucose transport regulated by CHH. As shown in Fig. 8, normal functioning of CHH in glucose transport relied on the existence of CHHBP, indicating that this hormone passed across the membrane through a ‘toll-gate’ molecule, CHHBP. On the basis of our colocalization results, we have no reason to doubt that CHHBP as a putative receptor at cell membrane is involved in the glucose metabolism and transport pathway regulated by CHH. Since we only analyzed the role of CHHBP under the control of CHH,

CHHBP is likely to be involved in numerous functions that have not yet been determined. In addition, it remains to be ascertained how CHHBP transduces the signal or whether it could it be a co-receptor for CHH. Thus, further exploration of the role of CHHBP must be undertaken to fully understand its function.

In conclusion, the results of the present study show that depletion of CHHBP leads to decreased blood glucose levels and glycogen storage in hepatic cells. CHHBP is involved in CHH-induced kinase cascades in crustaceans and interacts with CHH in the hepatopancreas. CHHBP probably acts as the primary signal processor of CHH-mediated regulation of cellular glucose metabolism.

Competing interests

The authors declare no competing or financial interests.

Author contributions

R.L. and J.-S.S. conceived the experiments and designed the research. R.L., J.-Z.T., C.-H.Z. and L.-N.Z. performed the experiments. R.L., J.-Z.T., C.-H.Z., X.-Y.G., Y.-C.Z. and J.-S.S. analyzed the data. R.L., J.-Z.T., C.-H.Z., Y.-C.Z. and J.-S.S. interpreted the results of the experiments. R.L. and J.-Z.T. prepared the figures. R.L. and J.-S.S. edited and revised the manuscript.

Funding

This work was supported by grants from the National High Technology Research and Development Program of China [2012AA10A401]; National Natural Science Foundation of China [31302168]; Natural Science Foundation of Tianjin [14JCYBJC30700]; Key Laboratory of freshwater aquaculture germplasm resources of Ministry of Agriculture: National Key Technology Program [2012BAD26B00] and Science and PhD Start-up Fund of Tianjin Normal University [52XB1303].

Data availability

The cDNA sequence for *CHHBP* is available from GenBank under accession number KJ700937.

References

Basu, A. C. and Kravitz, E. A. (2003). Morphology and monoaminergic modulation of crustacean hyperglycemic hormone-like immunoreactive neurons in the lobster nervous system. *J. Neurocytol.* **32**, 253-263.

Brix, A. E., Howertha, E. W., McConkie-Rosell, A., Peterson, D., Egnor, D., Wells, M. R. and Chen, Y. T. (1995). Glycogen storage disease type Ia in two littermate maltese puppies. *Vet. Pathol.* **32**, 460-465.

Chan, S.-M., Gu, P.-L., Chu, K.-H. and Tobe, S. S. (2003). Crustacean neuropeptide genes of the CHH/MIH/GIH family: implications from molecular studies. *Gen. Comp. Endocrinol.* **134**, 214-219.

Chung, J. S. and Webster, S. G. (2003). Moult cycle-related changes in biological activity of moult-inhibiting hormone (MIH) and crustacean hyperglycaemic hormone (CHH) in the crab, *Carcinus maenas*. From target to transcript. *FEBS J.* **270**, 3280-3288.

Chung, J. S. and Webster, S. G. (2006). Binding sites of crustacean hyperglycemic hormone and its second messengers on gills and hindgut of the green shore crab, *Carcinus maenas*: a possible osmoregulatory role. *Gen. Comp. Endocrinol.* **147**, 206-213.

Chung, J. S., Zmora, N., Katayama, H. and Tsutsui, N. (2010). Crustacean hyperglycemic hormone (CHH) neuropeptides family: functions, titer, and binding to target tissues. *Gen. Comp. Endocrinol.* **166**, 447-454.

Dai, J.-Q., Zhu, X.-J., Liu, F.-Q., Xiang, J.-H., Nagasawa, H. and Yang, W.-J. (2008). Involvement of p90 ribosomal S6 kinase in termination of cell cycle arrest during development of *Artemia*-encysted embryos. *J. Biol. Chem.* **283**, 1705-1712.

De Loof, A. (2008). Ecdysteroids, juvenile hormone and insect neuropeptides: recent successes and remaining major challenges. *Gen. Comp. Endocrinol.* **155**, 3-13.

Fecchi, K., Volonte, D., Hezel, M. P., Schmeck, K. and Galbiati, F. (2006). Spatial and temporal regulation of GLUT4 translocation by flotillin-1 and caveolin-3 in skeletal muscle cells. *FEBS J.* **20**, 705-707.

Hauser, F., Cazzamali, G., Williamson, M., Blenau, W. and Grimmelikhuijzen, C. J. P. (2006). A review of neurohormone GPCRs present in the fruitfly Drosophila melanogaster and the honey bee *Apis mellifera*. *Prog. Neurobiol.* **80**, 1-19.

Hauser, F., Cazzamali, G., Williamson, M., Park, Y., Li, B., Tanaka, Y., Predel, R., Neupert, S., Schachtner, J., Verleyen, P. et al. (2008). A genome-wide inventory of neurohormone GPCRs in the red flour beetle *Tribolium castaneum*. *Front. Neuroendocrinol.* **29**, 142-165.

Huang, X., Warren, J. T. and Gilbert, L. I. (2008). New players in the regulation of ecdysone biosynthesis. *J. Genet. Genomics* **35**, 1-10.

Kegel, G., Reichwein, B., Weese, S., Gaus, G., Peter-Katalinić, J. and Keller, R. (1989). Amino acid sequence of the crustacean hyperglycemic hormone (CHH) from the shore crab, *Carcinus maenas*. *FEBS Lett.* **255**, 10-14.

Kishnani, P. S., Faulkner, E., Vancamp, S., Jackson, M., Brown, T., Boney, A., Koeberl, D. and Chen, Y. T. (2001). Canine model and genomic structural organization of glycogen storage disease Type Ia (GSD Ia). *Vet. Pathol.* **38**, 83-91.

Lorenzon, S., Brezovec, S. and Ferrero, E. A. (2004). Species-specific effects on hemolymph glucose control by serotonin, dopamine, and L-enkephalin and their inhibitors in *Squilla mantis* and *Astacus leptodactylus* (crustacea). *J. Exp. Zool. A Comp. Exp. Biol.* **301A**, 727-736.

Lorenzon, S., Edomi, P., Giulianini, P. G., Mettulio, R. and Ferrero, E. A. (2005). Role of biogenic amines and cHH in the crustacean hyperglycemic stress response. *J. Exp. Biol.* **208**, 3341-3347.

Mohapatra, M., Sahu, N. P. and Chaudhari, A. (2003). Utilization of gelatinized carbohydrate in diets of *Labeo rohita* fry. *Aquac. Nut.* **9**, 189-196.

Montagné, N., Desdevises, Y., Soyez, D. and Toullec, J.-Y. (2010). Molecular evolution of the crustacean hyperglycemic hormone family in ecdysozoans. *BMC Evol. Biol.* **10**, 62.

Morrow, I. C., Rea, S., Martin, S., Prior, I. A., Prohaska, R., Hancock, J. F., James, D. E. and Parton, R. G. (2002). Flotillin-1/reggie-2 traffics to surface raft domains via a novel golgi-independent pathway: identification of a novel membrane targeting domain and a role for palmitoylation. *J. Biol. Chem.* **277**, 48834-48841.

Nagai, C., Nagata, S. and Nagasawa, H. (2011). Effects of crustacean hyperglycemic hormone (CHH) on the transcript expression of carbohydrate metabolism-related enzyme genes in the kuruma prawn, *Marsupenaeus japonicus*. *Gen. Comp. Endocrinol.* **172**, 293-304.

Nagai, C., Mabashi-Asazuma, H., Nagasawa, H. and Nagata, S. (2014). Identification and characterization of receptors for ion transport peptide (ITP) and ITP-like (ITPL) in the silkworm *Bombyx mori*. *J. Biol. Chem.* **289**, 32166-32177.

Reddy, P. S. and Kishori, B. (2001). Methionine-enkephalin induces hyperglycemia through eyestalk hormones in the estuarine crab *Scylla serrata*. *Biol. Bull.* **201**, 17-25.

Sedlmeier, D. (1987). The role of hepatopancreatic glycogen in the action of the crustacean hyperglycemic hormone (CHH). *Comp. Biochem. Physiol. A Physiol.* **87**, 423-425.

Sefiani, M., Le Caer, J.-P. and Soyez, D. (1996). Characterization of hyperglycemic and molt-inhibiting activity from sinus glands of the penaeid shrimp *Penaeus vannamei*. *Gen. Comp. Endocrinol.* **103**, 41-53.

Tavernarakis, N., Driscoll, M. and Kyrpides, N. C. (1999). The SPFH domain: implicated in regulating targeted protein turnover in stomatins and other membrane-associated proteins. *Trends Biochem. Sci.* **24**, 425-427.

Webster, S. G. (2015). Endocrinology of metabolism and water balance: crustacean hyperglycemic hormone. In *The Natural History of the Crustacea, Vol. 4, Physiology* (ed. E. S. Chang and M. Thiel), pp. 36-67. New York: Oxford University Press.

Webster, S. G., Keller, R. and Dircksen, H. (2012). The CHH-superfamily of multifunctional peptide hormones controlling crustacean metabolism, osmoregulation, moulting, and reproduction. *Gen. Comp. Endocrinol.* **175**, 217-233.

Yasuda, A., Yasuda, Y., Fujita, T. and Naya, Y. (1994). Characterization of crustacean hyperglycemic hormone from the crayfish (*Procambarus clarkii*): multiplicity of molecular forms by stereoinversion and diverse functions. *Gen. Comp. Endocrinol.* **95**, 387-398.

Yodmuang, S., Tirasophon, W., Roshorm, Y., Chinnirunvong, W. and Panyim, S. (2006). YHV-protease dsRNA inhibits YHV replication in *Penaeus monodon* and prevents mortality. *Biochem. Biophys. Res. Commun.* **341**, 351-356.

Zhao, F., Zhang, J., Liu, Y.-S., Li, L. and He, Y.-L. (2011). Research advances on flotillins. *Virol. J.* **8**, 479.

Žitňan, D., Kim, Y.-J., Žitňanová, I., Roller, L. and Adams, M. E. (2007). Complex steroid-peptide-receptor cascade controls insect ecdysis. *Gen. Comp. Endocrinol.* **153**, 88-96.